MAPPING OF TOTAL SUSPENDED SOLIDS CONCENTRATION IN PULICAT LAKE USING REMOTE SENSING

CREATIVE AND INNOVATIVE PROJECT REPORT

Submitted by

ANGELINE CHRISTY MOHANKUMAR

G.HARISHRI

N.ROJA

S.SHENAHA

In partial fulfillment for the award of the degree of

BACHELOR OF ENGINEERING

IN

GEOINFORMATICS ENGINEERING

DEPARTMENT OF CIVIL ENGINEERING

COLLEGE OF ENGINEERING GUINDY

ANNA UNIVERSITY: CHENNAI 600 025

OCTOBER 2016

ANNA UNIVERSITY: CHENNAI 600 025

BONAFIDE CERTIFICATE

Certified that this report titled **"MAPPING OF TOTAL SUSPENDED SOLIDS CONCENTRATION IN PULICAT LAKE USING REMOTE SENSING''** is a bonafide work of **ANGELINE CHRISTY MOHANKUMAR (2013107002), G.HARISHRI (2013107011), N.ROJA (2013107024)** and **S.SHENAHA (2013107028)** who carried the project work under my supervision for **GI 8711- Creative and Innovative Project.**

Dr.S.JAYALAKSHMI
Assistant Professor
Institute of Remote Sensing
Department of Civil Engineering
Anna University
Chennai – 600 025

ACKNOWLEDGEMENT

We would like to extend our sincere gratitude to our project guide **Dr.S.Jayalakshmi** Assistant Professor, Institute of Remote Sensing, for rendering help and guidance during the period of the project work and for her kind support.

We would like to thank **Dr. K. Nagamani**, Professor and Head, Department of Civil Engineering and **Dr.S.S.Ramakrishnan**, Director, Institute of Remote Sensing for providing us the opportunity to embark on this project

We would also like impart our deepest gratitude to **Mr.E.Velappan**, Associate Professor, Institute of Remote Sensing for his continued help and constant encouragement.

ANGELINE CHRISTY MOHANKUMAR
G.HARISHRI
N.ROJA
S.SHENAHA

ABSTRACT

Total Suspended Solids (TSS) is a primary indicator describing water quality because of its important influences on water bodies, such as transporting nutrients and contaminants, including heavy metals and micro-organisms. Pulicat Lake is the salt water lagoon and it is under threat due to pollution of fertilizers and pesticides from agriculture. Siltation is the major problem in Pulicat Lake. To map the TSS concentration, Polynomial Regression model was developed by correlating in situ total suspended solids and corresponding coordinate's pixel DN/indices value of Landsat 8 OLI/TIRS satellite data. Addition of Blue, SWIR2 and PAN bands in Landsat 8 OLI/TIRS image has the higher correlation with total suspended solids.

Results showed that TSS is higher in summer season compared to monsoon season and increasing every year. The region occupied by high TSS concentration in April is larger than in October for the year 2015 due to dilution of TSS caused by mild showers during October. The TSS ranges from 250 to 450 mg/l in the northern part of the lake and from 450 to 600 mg/l in the southern part of the lake for April 2015 and the concentration of TSS ranges from 0.0000001 to 250 mg/l in the northern part of the lake and from 400 to 600 mg/l in the southern part of the lake for October 2015. From April 2016, it is evident that the churning activity has led to the dispersion of high TSS concentration in the lake.

TABLE OF CONTENTS

LIST OF FIGURES

LIST OF TABLES

LIST OF ABBREVIATIONS

APHA-	American Public Health Association
AVHRR-	Advanced Very High Resolution Radiometer
CDOM-	Colored Dissolved Organic Matter
DO-	Dissolved Oxygen
ENVI-	Environment for Visualizing Images
HDPE-	High Density Polyethylene
LULC-	Land Use/ Land Cover
MODIS-	Moderate Resolution Imagery Spectroradiometer
NIR-	Near Infrared
NOAA-	National Oceanic and Atmospheric Administration
OLI-	Operational Land Imager
RS-	Remote Sensing
SNR-	Signal to Noise Ratio
SSC-	Suspended Sediment Concentration
SST-	Sea Surface Temperature
SWIR-	Short Wave Infrared
TIRS-	Thermal Infrared Sensor
TM-	Thermal Mapper
TSM-	Total Suspended Matter
TSS-	Total Suspended Solids
USGS-	United States Geological Survey

CHAPTER 1

INTRODUCTION

1.1 GENERAL

Coastal zone is a dynamic area with many cyclic processes owing to a variety of resources and habitats. Coastal lakes represent a tiny part (less than 1%) of the surface covered by oceans, but they are characterized by high biodiversity and intense primary productions, that lead to both ecological and economical considerable importance. Siltation and periodic closure of the bar mouth due to the dynamic process of sediment transport has caused reduction of size and seasonal closure of the mouth of the lake. This has reduced fresh sea water exchange and made the lake shallow and turbid. This has caused difficulties such as mouth getting silted up and getting closed during the summer season, raise in flood level occurs during the rainy season. The fluctuation of water level in the lake is affecting flora, fauna and fisheries.

Siltation has caused variation of the lake mouth resulting in the reduction of tidal inflows and consequent decline in stocking of commercially important species of prawns and mullets. The Arani and Kalangi rivers carrying runoff from agricultural fields in the drainage basin cause increase in pollution load from fertilizers and pesticides into the lake. Lake is further polluted due to domestic

sewage, effluents and wastes from numerous fish processing units, oil spills from the mechanized boats, petrochemical complex, power plant and satellite port in Ennore. This study is aimed to estimate total suspended solids in Pulicat Lake.

Suspended solids consist of an inorganic fraction (silts, clay, etc.) and an organic fraction (algae, zooplankton, bacteria etc.) that are carried along by water as it runs off the land. When the suspended particles settle down to bottom, it causes the sediment or silt. Estimates of total suspended solids using remote sensing technique is an efficient method.

1.2 NEED FOR STUDY

The current conventional techniques for measuring water quality variables are time consuming and do not give a synoptic view of water body or more significantly, a synoptic view of different water bodies across the landscape. It requires expensive laboratory analysis, especially for a large area. Thus it is very difficult to report and predict the water quality situation in time. With the development of remote sensing (RS) techniques, water quality monitoring based on RS methods becomes accessible and very efficient. Remote sensing methods used frequent, inexpensive and continuous monitoring of water quality parameters over large spatial extent. Remote sensing techniques optimize the sample strategy and time.

1.3 OBJECTIVE OF THE STUDY

The main objectives of this study are:

1. To develop Landsat 8 OLI/TIRS based TSS retrieval regression models.
2. To retrieve Total Suspended Solids from satellite data
3. To generate spatial temporal changes of TSS in Pulicat lake.

1.4 ORGANISATION OF THE REPORT

This report is organized as six chapters. In Chapter 1, the general introduction followed by the need for study are given. The concepts observed from review of journals are discussed in Chapter 2. Chapter 3 and 4 describes about study area details and materials and methods respectively. Chapter 5 contains results and discussions obtained from analysis and Chapter 6 gives the summary and conclusions for the study.

CHAPTER 2

LITERATURE REVIEW

2.1 GENERAL

Chunlei Fan (2014) developed algorithms for hyperspectral remote sensing of water quality based on in situ spectral measurement of water reflectance. In this study, water reflectance spectra R (λ) were acquired by a pair of Ocean Optic 2000 Spectroradiometers during the summers from 2008 to 2011 at Patuxent River, a tributary of Chesapeake Bay, USA. Simultaneously, concentrations of TSS as well as absorptions of coloured dissolved organic matter (CDOM) were measured. Empirical models that are based on spectral features of water reflectance generally showed good correlations with water quality parameters. The ratio of green and blue spectral bands is the best predictor for TSS (R^2 =0.75) and CDOM absorption is best correlated with spectral features at blue and NIR regions (R^2 = 0.85). These empirical models were further applied to the ASIA Eagle Hyperspectral aerial imagery to demonstrate the feasibility of Hyperspectral remote sensing of water quality in the optical complex estuarine waters.

This work concluded that Hyperspectral remote sensing can capture a more comprehensive picture of water quality than is obtained by a conventional ground-based monitoring program. However, to make this feasible, the *in situ*

spectral measurement is a critical step toward retrieval model development. Because of the spectral features of water reflectance by different water quality parameters, the band selection or model development should focus on these wavelength regions for retrieval of such optical constituents. It was found that the ratio of red and green spectral region is best for TSS prediction, and the CDOM absorption was found to be correlated with the spectral features in NIR and blue regions. These developed algorithms can be further applied to hyperspectral images to generate detailed water quality maps for ecosystem monitoring and managements. However, the coefficients in these retrieval models were derived from the dataset that is specific to the study area, so do not necessarily represent the coastal waters in other areas. The accuracy of such algorithms is always subject to the location of ground truthing dataset.

Lijuan Cui et al. (2013) applied Moderate Resolution Imaging Spectroradiometer (MODIS) images from 2000 to 2010 to obtain and analyze the spatiotemporal variation of suspended sediment concentration (SSC) and discussed factors affecting it in Poyang Lake. This study aimed to develop MODIS-based SSC retrieval models and apply the developed models to retrieve SSC from MODIS images.

Results showed that (1) the mean SSC was lower in the south, higher in the north, and moderate in the central lake region; (2) the mean SSC in the south was lower than or close to 20 mg/L, with no clear annual trend; (3) the mean SSC in the north was slightly higher than 20 mg/L in 2000 and increased from 2001, with the highest value >60 mg/L in 2006; (4) the mean SSC in the central lake region, except for 2009, ranged from 20 to 40 mg/L and had an annual pattern similar to that in the southern lake region; (5) for the entire lake, the mean SSC

declined from January to March, increased from September to December, and fluctuated from April to August; and (6) several higher SSC values were found in the central or southern lake regions. The spatiotemporal variation of SSC was controlled by natural and human factors, in which dredging was dominant.

Limiting the area of dredging and reducing dredging intensity would decrease SSC and maintain sustainable development of Poyang Lake. Remote sensing can obtain the spatiotemporal information of some water quality parameters, which will help managers understand the lake dynamics and mechanisms to make better decisions for lake management.

The distance between 2 adjacent sampling points was >1.5 km, and thus one pixel of MODIS image with 250 m spatial resolution at most covers one sampling point. The spectral values at each sampling point were assumed equal to those of the pixel in which the sampling point is located, and thus 54 SSC measurements in 2007 and 2010 combined with their corresponding MODIS Terra 250 m red and infrared band reflectance were used to develop the best-fitting model for estimating SSC from MODIS Terra image. The descriptive statistics of SSC and red and infrared band reflectance were performed first. The linear, logarithmic, quadratic, cubic, power, growth, and exponential models between the SCC and the single red or infrared band, or the ratio or difference of the 2 bands were then calibrated, respectively, with the least-squares technique to find the best-fitting model for SSC estimation. Finally, the determination coefficients (R^2) and estimated standard errors (SE) of all the calibrated models were compared to determine the best-fitting model. The best-fitting model was validated using the leave-one-out cross-validation (LOOCV) technique.

Abdullah et al. (2009) has carried out a study on monitoring of total suspended solids and sea surface temperature using NOAA- AVHRR data. In this study, the National Oceanic and Atmospheric Administration Multi Channel Sea Surface Temperature (NOAA MCSST) algorithm was used to determine the sea surface temperature (SST) by using NOAA AVHRR data. This study is included remote sensing of total suspended solids (TSS) on the surface of water.

AVHRR radiometric correction and calibration, the DN values were converted into radiance and reflectance values. The reflectance values acquired from the ground truth sample locations were extracted from all the images. In order to minimize the atmospheric effects within multi-temporal data, the correction was performed between the scenes. The results revealed that the data set produced higher correlation coefficient and lower RMS value for window size of 3 by 3, in terms of reflectance values. Therefore, it was used in this study. Finally, an automatic geocoding technique from PCI Geomatica 9.1.8 -AVHRR Automated Geometric Correction was applied in this study to geocode the SST and TSS maps.

Jining Chen et al. (2008) performed water quality monitoring in slightly polluted inland water body through remote sensing. The main objective of the study is deriving water quality retrieval models for eight common water quality variables, including algae content, turbidity and concentrations of chemical oxygen demand, total nitrogen, ammonia nitrogen, nitrate nitrogen, total phosphorus and dissolved phosphorous by using Landsat 5 Thematic Mapper (TM) data using multiple regression methods.

Three groups of algorithms were applied for water quality retrieval from RS data, i.e., empirical algorithms, theoretic algorithms, and their combinations. Due to the complexity of the theory and the difficulty of calculation, many people were still using empirical algorithms. This study used multiple linear regression algorithm, the most famous empirical one, to establish the correlation between RS data and water quality variables. Stepwise multiple linear regression was applied to find the best correlation with the entry significance at a level of 0.05 and the removal significance at a level of 0.10. Finally the regressive model should pass the F test at the confidence level of 95%.

In order to find the best sampling method of pixel DNs for water quality retrieval, three different ways were tried to use pixel DNs, which are the original single pixel DN, the average and median values of a 3×3 pixel window. Eight water quality variables and their natural logarithms were all selected to be the dependent variables for regression. For the independent variables, besides DNs, the DN's reciprocals, squares, square roots, powers of *e* and the ratio of each two bands' DNs were also considered. With stepwise multiple linear regression using original DNs, seven water quality variables can get satisfied regressive correlations except COD. In this study, COD could not be retrieved under a degree of confidence at 90%.

The significances of the regressive retrieval models indicated that there existed a statistical perfect correlation for water quality variables including algae content, turbidity, and concentrations of TN, NH3-N, TP, and DP to Landsat-5 TM data, while COD could not be retrieved within an acceptable error in this study. The correlation coefficients of the seven regressive equations were fairly

high, among which four coefficients were higher than 0.9, only those of TN and TP were lower than 0.8.

The results showed that there existed a statistical significant correlation between each water quality variable and remote sensing data in the slightly-polluted inland water body with fairly weak spectral radiation. With appropriate method of sampling pixel digital numbers and multiple regression algorithms, algae content, turbidity, and nitrate nitrogen concentration could be retrieved within 10% mean relative error, concentrations of total nitrogen and dissolved phosphorus within 20%, concentrations of ammonia nitrogen and total phosphorus within 30% while chemical oxygen demand had no effective retrieval method. These accuracies were acceptable for the practical applications of routine monitoring and early warning on water quality safety with some support of precise traditional monitoring. The results showed that it was possible and effective to perform most traditional routine monitoring tasks of water quality on relatively clean inland water bodies by RS.

Dekkera et al. (2001) performed this study on comparison of remote sensing data, model results and in situ data for total suspended matter (TSM). Synoptic information on suspended matter at a regular frequency is difficult to obtain from the routine in situ monitoring network since suspended matter is a spatially inhomogeneous parameter. Landsat 5 TM and SPOT HRV data were atmospherically corrected and converted to total suspended matter maps. The algorithms are based on analytical optical modelling, using the in situ inherent optical properties. This methodology enables the development of multi-temporal algorithms for estimating seston dry weight concentration in lakes from remotely

sensed data; thus satellite data can now become an independent measurement tool for water management authorities.

A problem in this study was that the total suspended matter content for several of the larger lakes was absent from the standard monitoring database of Waterschap Friesland for 1995. As a consequence, no standard in situ TSM information is available for comparison with remote sensing results. Satellite systems give important additional information on spatial trends observed in suspended matter and transparency. This information must be taken into account in the future for a more realistic trend analysis. The remote sensing patterns demonstrate clearly the often poor representability of a point sample for the whole lake.

Remote sensing information may help to obtain more representative monitoring locations of suspended matter and related parameters as chlorophyll and Secchi disk depth. An overall conclusion from this study was that the combined use of water quality model results, satellite remote sensing data and in situ data leads to better monitoring and understanding of suspended matter and transparency in the southern Frisian lakes.

Buttner et al. (1987) investigated suitability of satellite remote sensing to map chlorophyll-A. Suspended materials distribution for a lake and a reservoir. Stepwise linear regression analysis has been applied to derive relationship between satellite measured radiances and in situ water quality data. In spite of the mixing effects of chlorophyll-A absorption and reflection of suspended particles on radiances, good correlations (R=0.71-0.90) were obtained between Landsat MSS and reference measurements. A method for reliability assessment

of a regression equation was applied based on the analysis of correlation coefficient and standard error of estimate obtained for randomly partitioned data.

The regression equations, developed between the water quality measurements and the mean radiances obtained from Landsat CCT, were extended to the entire water areas for mapping the selected water quality parameters. By applying the regression equation to each pixels in the study area and then linearly slicing the result into 3-5 discrete water quality classes, the classification was accomplished. Colour coded maps were produced, which were converted to black and white illustrations.

Reliability assessment of water quality maps is difficult to make. As all the samples were used for the development of the best regression equation possible, no samples remained for testing. The following experiment was carried out to test the results obtained for case BI. The 42 element sample set was partitioned randomly into training and test subsets. There were ten different groups for each of the training subsets, considering of 37, 32, 28, 21 and 14 samples.

Training samples were used to compute regressions using variables. The average correlation coefficients (R) are decreasing with the sample number of both water quality parameters. This change is smaller for chlorophyll-a, which indicate a more stable determination of this variable. Test samples were used to calculate the standard error of estimate (SEE) for each of the regression equations obtained for the training data subsets. The crosses mean SEE values obtained by using all the 42 samples for testing. For chlorophyll-a the average

SEE has an increasing tendency with the number of test samples, according to expectation. The behavior of the SEE values for suspended materials however difficult to explain. The 50% difference between mean SEE obtained for 5 test samples and that of whole data set indicates some instability of the related regression equation.

The reservoir is characterized by low chlorophyll-a values and very high suspended sediment concentrations, due to the high water running down on the River Tisza. The chlorophyll-a and sediment concentrations are uncorrelated. Both water quality parameters are explained fairly well by a single Landsat band: Chlorophyll-a is correlated by MSS1 (R = 0.87), while suspended material is correlated. The reservoir is characterized by substantially lower sediment concentration and a higher chlorophyll-a concentration compared to the K I case. The two water quality measurements are correlated. The correlation coefficients for the regressions are poorer than in the KI case (R = 0.71 for chlorophyll-a and R = 0.72 for suspended materials). Chlorophyll-a distribution is explained by the weighted difference of MSS3 and MSS2 values with nearly equal explaining potential. Suspended materials are given by the weighted difference of MSS3 and MSS1, putting bigger weight to the former band.y MSS4 (R = 0.86).

The correlation between satellite radiances and *in situ* water quality data is between 0.71 and 0.90 for two different types of inland waters and for two different dates. Satellite data can explain 50-80% of the measured variances, in spite of the mixing effect of chlorophyll absorption and reflection of suspended particles in the water. The correlation between satellite data and chlorophyll-a measurements is slightly better than that of between satellite and suspended material data. Reliability assessment made for one of the cases has shown, that

the regression relation for chlorophyll-a is more stable, than for the suspended materials.

2.2 INFERENCE FROM LITERATURE REVIEW

Most of the studies have developed water quality algorithms by correlating in situ measurements and the remote sensing data. Total suspended solids is a primary indicator of water quality study in lakes. This study aims to develop regression model to estimate Total suspended solids using field measurements and satellite data.

CHAPTER 3

STUDY AREA

3.1 GENERAL

The Pulicat lake boundary limits range between 13.33°N to 13.66° N and 80.23°E to 80.25°E, with a dried part of the lake extending up to 14.0°N; with about 96% of the lake in Andhra Pradesh and 3% in Tamil Nadu (Figure 3.1). The lake is aligned parallel to the coast line with its western and eastern parts covered with sand ridges. Area of the lake varies with the tide; 450 square kilometers (170 sq mi) in high tide and 250 square kilometers (97 sq mi) in low tide. Its length is about 60 kilometers (37 mi) with width varying from 0.2 kilometers (0.12 mi) to 17.5 kilometers (10.9 mi). Climate of the lake coast line is dominated by Tropical monsoons. Air temperature varies from 15 °C (59 °F) to 45 °C (113 °F).

Two rivers which feed the lake are the Arani River at the southern tip and the Kalangi River from the northwest, in addition to some smaller streams. The Buckingham Canal, a navigation channel, is part of the lake on its western side. The lake's water exchange with the Bay of Bengal is through an inlet channel at the north end of Sriharikota and out flow channel of about 200 meters (660 ft) width at its southern end, both of which carry flows only during the rainy

season. The lake acts as buffer to retain the accumulated flood water till the flood water is discharged gradually to the sea during the monsoon period and cyclones.

The water quality of the lake varies widely during various seasons – summer, pre–monsoon, monsoon and post–monsoon – as the depth and width of the lake mouth varies causing a dynamic situation of mixing and circulation of waters. The resultant salinity variation and DO (dissolved oxygen) affects the primary production, plankton, biodiversity and fisheries in this lake.

The benthic or the bottom habitat of this lake is classified into three zones. The southern zone, the first zone, is dominated by sand with some admixture of mud. The second zone at the northern region is wholly muddy. The third zone with sand and mud in equal parts is overgrown with patches of weeds and is reported to be rich in benthic biodiversity.

3.1.1. BIODIVERSITY OF PULICAT LAKE

Pulicat Lake is one of the good productive ecosystems in India. Chacko et al. (1953) have given the first exhaustive account of the biodiversity of the Pulicat Lake. Chacko et al. (1953) have recorded 59 species of phytoplankton and 23 species of zooplankton, but Krishnan and Sampath (1973) have recorded much less, only 16 phytoplankton, but more zooplankton, 35 species. Today, it is still

less in numbers. Mid 1970s, when shrimp from the Pulicat Lake started, the White shrimp (*Penaeus indicus*) has literally become the "White Gold" at Pulicat.

Although Chacko et al. (1953) recorded only 4 species of shrimps from the Pulicat Lake, yet later Paul Raj (1976) recorded 12 species from the lake. Six of them, *Penaeus indicus, P. monodon, P. semisulcatus, Metapenaeus dobsoni, M. affinis and M. brevicornis* are more common, of which *P. indicus* is the most dominant species in the lake sustaining a major fishery and export trade at Pulicat. The mud crab or green crab, as it is variously called, is reputed from the Pulicat Lake since ancient times.

STUDY AREA

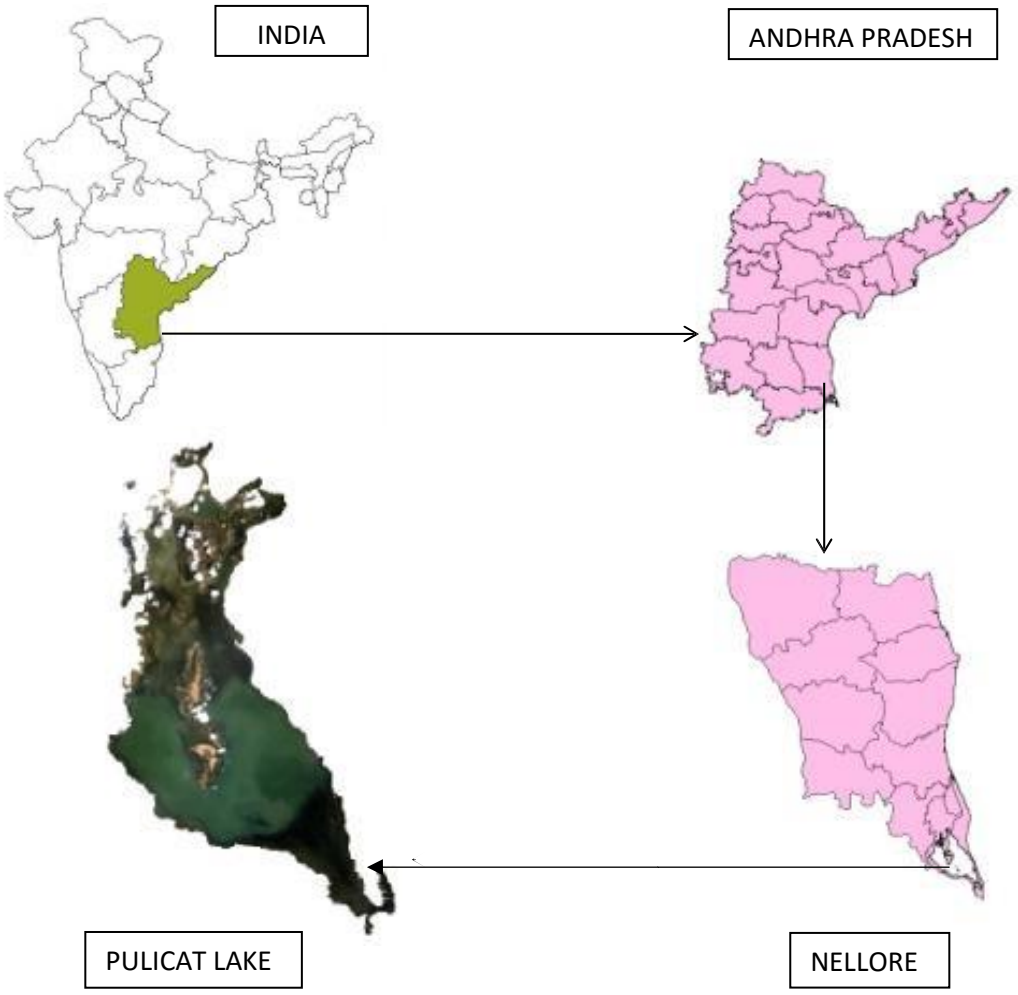

Fig 3.1- Study Area

CHAPTER 4

MATERIALS AND METHOD

4.1 FLOW CHART

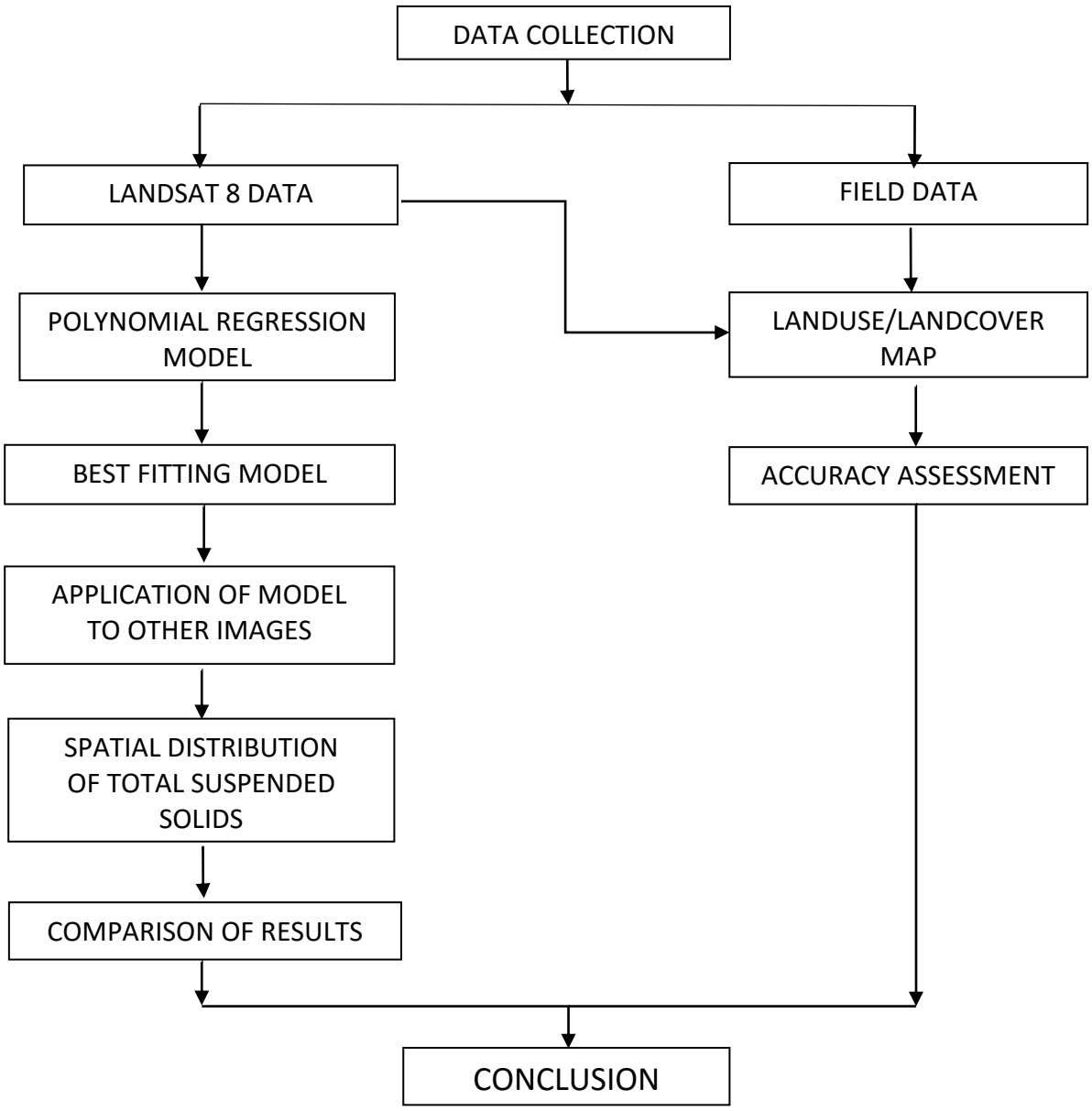

Fig 4.1 Flow Chart of Methodology

Figure 4.1 shows the methodology followed for mapping the TSS concentration in Pulicat Lake in the form of a flow chart.

4.2 DATA COLLECTION

The 32 representative water samples were collected from Pulicat Lake on the date 26.09.14 for the area of interest. The corresponding Landsat 8 OLI/TIRS satellite data was also collected. Water samples were taken randomly at 32 sampling sites from the southern part of Pulicat Lake. Water samples were taken more in settlements, industries and agricultural activities are highly associated with the Pulicat Lake.

The co-ordinates of sampling sites were obtained through hand held GPS. The sampling and chemical analysis were based on Standard Method .The Landuse/Landcover map for the study area was prepared using supervised classification method of maximum likelihood.

4.3 LANDUSE AND LANDCOVER

Landsat 8 OLI/TIRS is used to prepare Land Use/Land Cover map for Pulicat Lake. First the unsupervised classification using isodata algorithm was performed to classify the image into 20 classes to identify different features available in the image. However the unsupervised classification gives

misclassification. The supervised classification has to be performed. Representative training sites of each class such that Waterbody, Vegetation, Scrub land, Wetland, Sandy Area and Settlements within the Landsat 8 image has been selected. Signature file contains spectral statistics for each pixel found within each training site. These training sites were used for the supervised classification using Maximum likelihood algorithm in the ERDAS IMAGINE software.

4.4 ACCURACY ASSESSMENT FOR LAND USE/ LAND COVER

The kappa coefficient of agreement is frequently used to summarize the results of an accuracy assessment used to evaluate land-use or land-cover classifications obtained by remote sensing. The standard estimator of the kappa coefficient along with the standard error of this estimator require a sampling model that is approximated by simple random sampling.

Kappa analysis is a discrete multivariate technique of use in accuracy assessment. An estimate of Kappa is a measure of agreement or accuracy. The equation of Kappa statistics

$$K_{hat} = \frac{N \sum_{i=1}^{r} x_{ii} - \sum_{i=1}^{r} (x_i * x_{+i})}{N^2 - \sum_{i=1}^{r} (x_{i+} * x_{+i})}$$

Where

r= No. of rows in the matrix

x_{ii} = Total no. of corrected cells (i.e. value in row i and column i)

x_{i+}= Total for row i

x_{+i}= Total for column i

N= Total no. of cells in error matrix

4.5 SAMPLING DESIGN

The 32 samples were collected from the southern part of Pulicat Lake is shown in the Figure 4.2. Sampling location interval distance is more than 30m that is, it is more than spatial resolution of Landsat 8 OLI/TIRS satellite data.

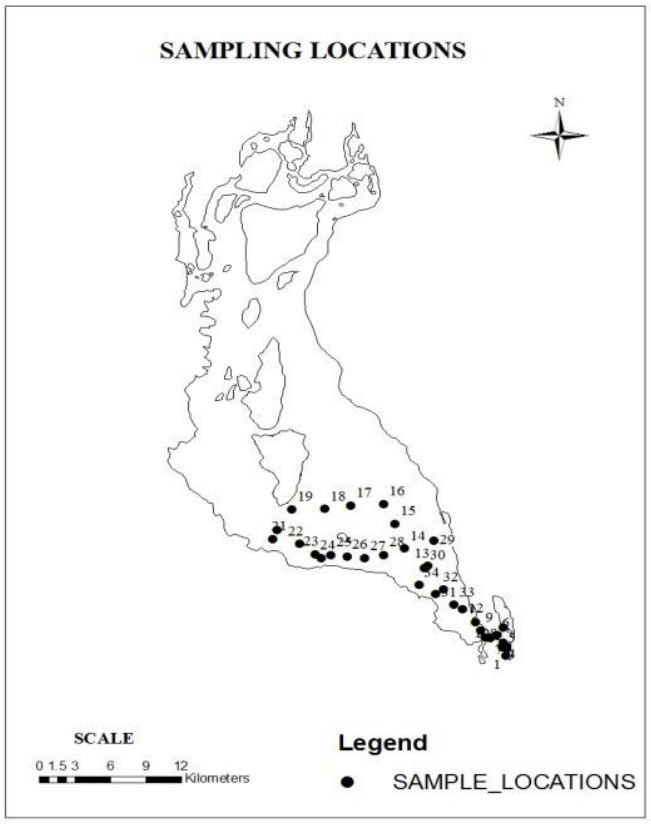

Fig 4.2-Sample Points

4.6 REMOTE SENSING DATA

The Landsat 8 OLI/TIRS images were downloaded from USGS Earth Explorer website. Landsat 8 image is acquired on 9thSeptember 2014, on the date closest to field study data with least cloud cover.

Landsat 8 carries two instruments-

- The Operational Land Imager (OLI) sensor includes refined heritage bands along with three new bands, a deep blue band for coastal/ aerosol studies, a shortwave infrared band for cirrus detection and a Quality Assessment band.
- The Thermal Infrared Sensor (TIRS) provides two thermal bands.

The sensors both provide improved Signal-to-Noise Ratio (SNR) radiometric performance quantized over a 12-bit dynamic range. It has a repetitive period of 16 days. The spatial and spectral resolutions and the use of various bands of Landsat 8 are given below (Table 4.1):

TABLE 4.1- DIFFERENT BANDS OF LANDSAT 8 OLI/TIRS

Band	**Wavelength**	**Useful for mapping**
Band 1 – coastal aerosol	0.43 - 0.45	Coastal and aerosol studies
Band 2 – blue	0.45 - 0.51	Bathymetric mapping, distinguishing soil from vegetation and deciduous from coniferous vegetation
Band 3 – green	0.53 - 0.59	Emphasizes peak vegetation, which is useful for assessing plant vigour
Band 4 – red	0.64 - 0.67	Discriminates vegetation slopes
Band 5 - Near Infrared (NIR)	0.85-0.88	Emphasizes biomass content and shorelines
Band 6 - Short-wave Infrared (SWIR) 1	1.57 - 1.65	Discriminates moisture content of soil and vegetation; penetrates thin clouds
Band 7 - Short-wave Infrared (SWIR) 2	2.11 - 2.29	Improved moisture content of soil and vegetation and thin cloud penetration
Band 8 – Panchromatic	0.50 - 0.68	15 meter resolution, sharper image definition
Band 9 – Cirrus	1.36 - 1.38	Improved detection of cirrus cloud contamination
Band 10 – TIRS 1	10.60 – 11.19	100 meter resolution, thermal mapping and estimated soil moisture
Band 11 – TIRS 2	11.5 - 12.51	100 meter resolution, Improved thermal mapping and estimated soil moisture

(Source: http://landsat.usgs.gov/best_spectral_bands_to_use.php, visited on 25.10.16)

4.7 SAMPLE DATA ANALYSIS

The containers that were used for sample collection for this study were made of high density polyethylene (HDPE), polypropylene, polycarbonate or a fluoropolymer. The sample bottles were cleaned before final collection of water sample as it is important not to increase the turbidity of water while collecting the sample. Excessive turbulence was also avoided to minimize the presence of air bubbles in the water while sample collection. Sample water was filled up to the shoulder of the bottle. Water samples were refrigerated at 1-4 º C, and were analyzed within 24 hours.

4.8 TOTAL SUSPENDED SOLIDS

TSS are solid materials, including organic and inorganic, that are suspended in the water. The standard Gravimetric Method (APHA. 2012) is followed for measuring the Total Suspended Solids (TSS). TSS is defined as the portion of total solids in a water sample retained by a glass fibre (GF/C) filter of pore size 0.45 micrometre. Water sample was filtered through a glass fibre (GF/C) filter of nominal pore size of 0.45 micrometre.

Once the filter has been dried at 103- 105º C and weighed, the amount of Total Suspended Solids is recorded in units of mg/L. TSS for each sample was calculated using the following equation:

TSS (mg/L) = [(A-B)*1000]/ mL Sample

Where,

A= Weight of filter+ dried residue in mg

B= Weight of Filter

4.9 REGRESSION MODEL DEVELOPMENT

Regression analysis estimates the conditional expectation of the dependent variable given the independent variables – that is, the average value of the dependent variable when the independent variables are fixed. The regression model was developed by correlating measured Total suspended solids and the corresponding pixel DN values. The DN values were taken as the independent variables and the Total suspended solids concentration values that were obtained by sample collection was taken as the dependent variable. The regression model was developed using the Data Analysis tool in Microsoft excel. The scatter plot was generated and a trend line was added to the plot with an order of six. The regression was applied for many band combinations and the combination band 2+7+8 which gave the higher correlation coefficient close to 1 was chosen as the regression model equation for further studies. The determination of co-efficient from the best equation was noted down.

4.9.1 LINEAR REGRESSION MODEL

Linear regression is an approach for modelling the relationship between a scalar dependent variable y and one or more explanatory variables

denoted X variables denoted X. The case of one explanatory variable is called simple linear regression.

The equation of simple linear regression is shown in the following equation

y= a+bx

Where,

a- Intercept of the line

b- Slope of the line

y- Dependent variable is total suspended solids

x- Independent variable

In this model DN values of each band or index has taken as independent variable and total suspended value has taken as dependent variable. The independent variables are tabulated in table given below:

Coefficient of determination R^2 = (SSE-SST)/ SST

Standard Error= Square root [SSE/ (n-2)]

Where,

SST= Total variability

SSR= Sum of Squares due to regression

SSE= Sum of Squares due to error

n= number of samples used for regression model

4.9.2 POLYNOMIAL REGRESSION MODEL

In statistics, polynomial regression is a form of linear regression in which the relationship between the independent variable x and the dependent variable y is modelled as an nth degree polynomial. Polynomial regression fits a nonlinear relationship between the value of x and the corresponding conditional mean of y, denoted E(y | x), and has been used to describe nonlinear phenomena such as the growth rate of tissues, the distribution of carbon isotopes in lake sediments, and the progression of disease epidemics. Although polynomial regression fits a nonlinear model to the data, as a statistical estimation problem it is linear, in the sense that the regression function E(y | x) is linear in the unknown parameters that are estimated from the data. For this reason, polynomial regression is considered to be a special case of multiple linear regression.

In general, we can model the expected value of y as an nth degree polynomial, yielding the general polynomial regression model

$$\mathbf{y = a}\boldsymbol{a_0} + \boldsymbol{a_1 x} + \cdots + \boldsymbol{a_n x^n}$$

4.10 ANALYSIS IN ENVI

Band Math is a flexible image processing tool with many capabilities not available in any other image processing system. The Band Math dialog can be used to define bands or files used as input, to call a user Band Math function, and to write the result to a file or memory.

The Band Math function accesses data spatially by mapping variables to bands or files. Spatial data that are too large to read entirely into memory are automatically accessed using data tiling. The sixth order polynomial empirical regression model that was developed was applied to the images of the year 2015 and 2016 using Band Math tool in ENVI.

The following Figure 4.3 depicts Band Math processing that adds three bands. Each band in the expression is mapped to an input image band, summed, and output as the resulting image data. For example, in the expression b1 + b2 + b3, if b1 is mapped to a file and b2 and b3 are mapped to a single band, then the resulting image file contains the bands of the b1 file summed with b2 and b3.

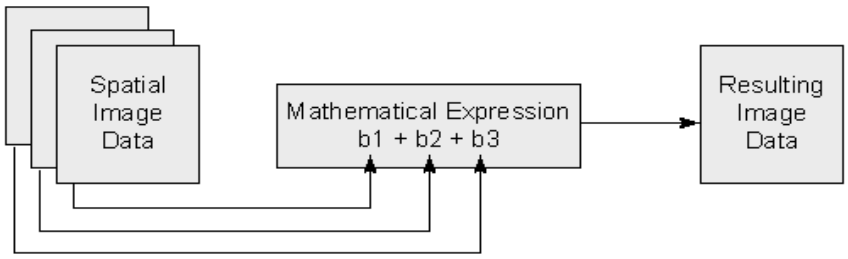

Fig 4.3- Band Math in ENVI

CHAPTER 5

RESULTS AND DISCUSSIONS

5.1 LAND USE AND LAND COVER MAP

The Land Use and Land Cover map (Figure 5.1) for the study area and the area covered in meters (Table 5.1) is shown below. The southern part of the Pulicat Lake is mostly influenced by settlements and vegetation. These are main sources of pollution to the lake.

Accuracy assessment is carried out for the classification map using Google earth data. Error matrix and accuracy report of Land use and Land Cover map is calculated. Over all accuracy of the classification map is 90 % and Kappa coefficient is 91.7%

TABLE 5.1- AREA COVERED BY VARIOUS FEATURES

Serial No.	Feature	Area in Meters
1	Wetland	251671500
2	Vegetation	1632603600
3	Scrubland	90336600
4	Water	1333665000
5	Sandy Area	287544600
6	Settlements	631922400

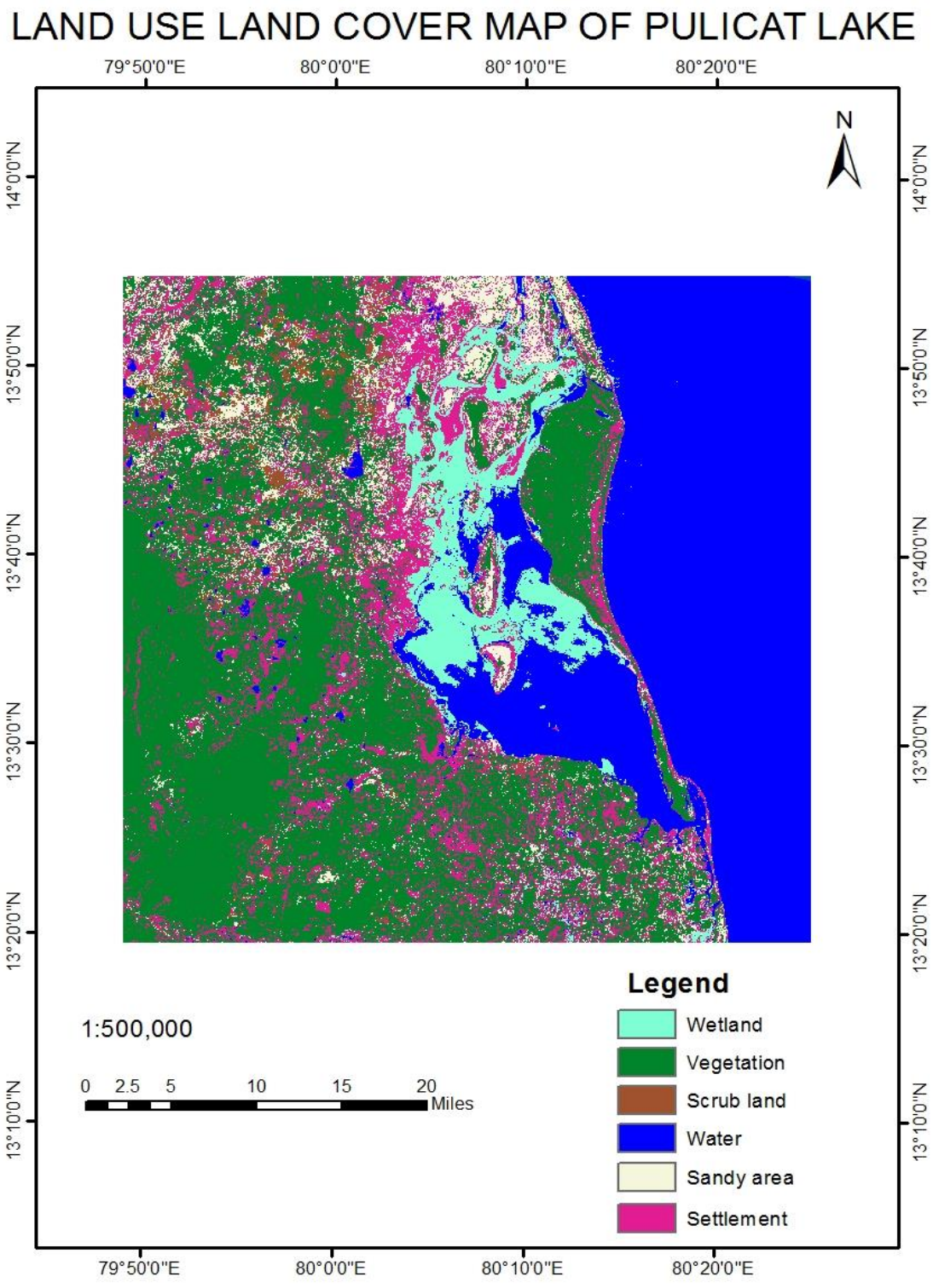

Fig 5.1- LU/LC Map of Pulicat Lake

From the Land use and Land Cover map, it is evident that the vegetation covers a major area of about 1,632,603,600 m^2, while scrub land occupies the minimum area of about 90,336,600 m^2. Area covered by Pulicat Lake and the other small water bodies is 1,333,665,000 $m^{2.}$.

From the Error Matrix (Table 5.2) for the classification map, it can be seen that the classes of vegetation, scrub land, sandy areas and water are perfectly classified whereas wetland and settlements have some wrongly classified pixels.

TABLE 5.2- ERROR MATRIX OF CLASSIFICATION MAP

Classification	Wetland	Vegetation	Scrubland	Water	Sandy Area	Settlements	Row Total
Wetland	3	0	0	1	0	0	4
Vegetation	0	2	0	0	0	0	2
Scrubland	0	0	2	0	0	0	2
Water	0	0	0	4	0	0	4
Sandy area	0	0	0	0	4	0	4
Settlements	0	0	0	0	1	3	4
Column Total	3	2	2	5	5	3	20

From Table 5.3, we can infer that the Producer's Accuracy for the classes – Wetland, vegetation, scrubland and settlements is 100% while that of water and

sandy area is 80%. The User's Accuracy for vegetation, water, scrubland, sandy area is 100% while that of wetlands and settlements is 75%.

TABLE 5.3 -ACCURACY REPORT OF LAND USE AND LAND COVER MAP

Serial No	Class Name	Reference Total	Classified total	Number Correct	Producer's Accuracy	User's Accuracy
1	Wetland	3	4	3	100	75
2	Vegetation	2	2	2	100	100
3	Scrubland	2	2	2	100	100
4	Water	5	4	4	80	100
5	Sandy Area	5	4	4	80	100
6	Settlements	3	4	3	100	75

5.2 DRAINAGE MAP

The drainage map shown in Figure 5.2 has been prepared from google earth base map. It shows three main rivers –Arani, Kalanji, Swarnamukhi draining into Pulicat Lake. It is observed that the TSS concentration is higher at the river inlets.

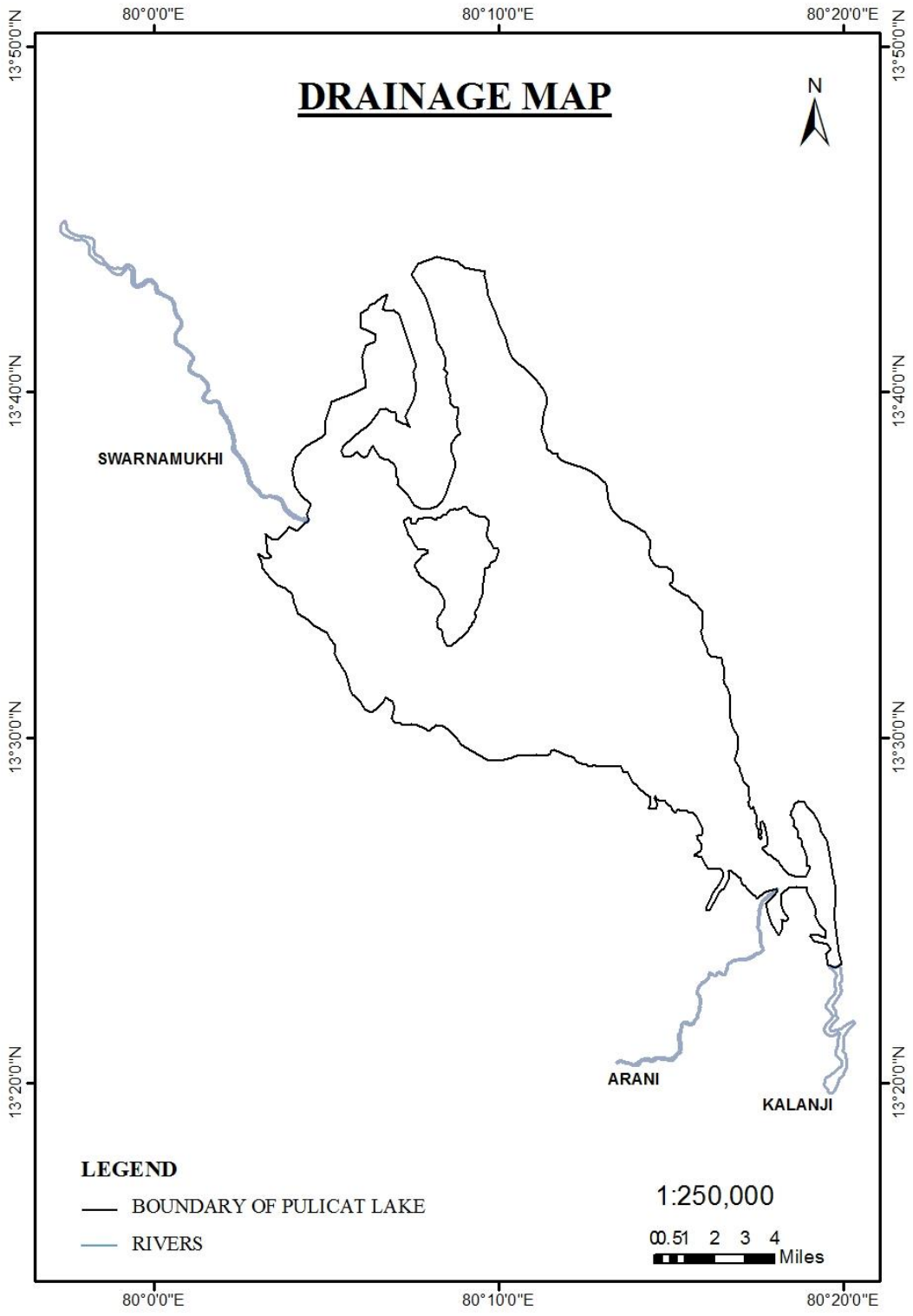

Fig 5.2- Drainage Map of Pulicat Lake

5.3 BATHYMETRY OF PULICAT LAKE

The bathymetry data was downloaded from National Oceanography Centre website- General Bathymetric Chart of Oceans (GEBCO). The study area subset was created from the downloaded data and then was resampled using the resampling tool available in Raster Processing in Arc Tool box. Fig 5.3 shows the Bathymetric Map of Pulicat Lake which gives the height from Mean Sea Level at all points of the lake. It can be observed that the height changes from -8.238 m to 2.003 m.

5.4 TOTAL SUSPENDED SOLIDS

Table 5.4 shows the 32 sample point locations in latitude and longitude along with the total suspended solids concentration at those points. The total suspended solids measured from the laboratory analysis are shown in the Table 5.4. The TSS in Pulicat Lake ranges from 9mg/l to 162mg/l.

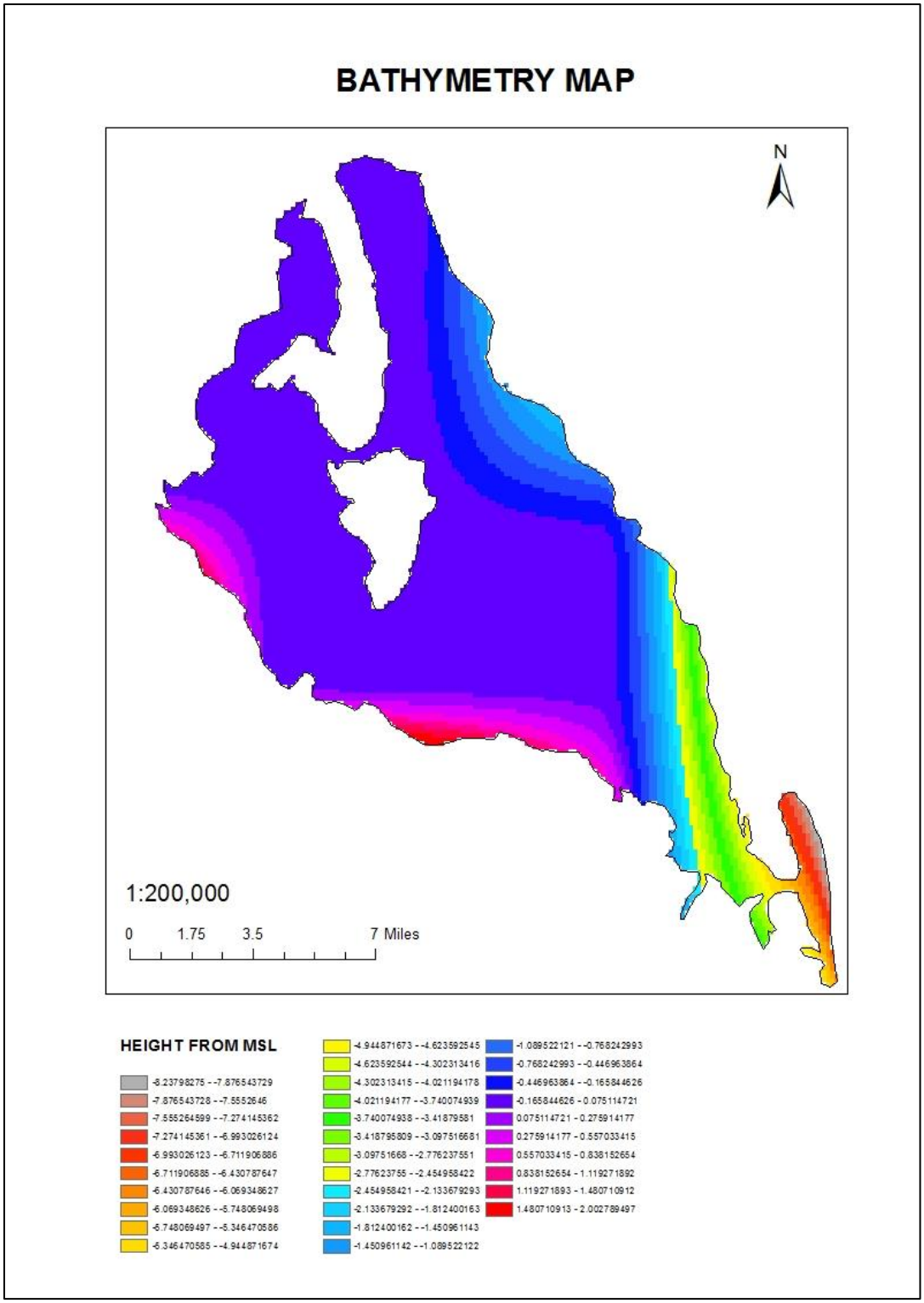

Fig *5.3- Bathymetry of Pulicat Lake*

5.5 REGRESSION MODEL ANALYSIS

The regression models were developed by correlating measured total suspended solids and corresponding pixel DN values using Data Analysis tool in Microsoft Excel. The correlation co-efficient for the equations were obtained.

It was observed that order 6 empirical regression equations gave better accuracy i.e. R^2 values were closer to 1.The calibrated models were compared to determine the best fitting model.

Table 5.5 shows the polynomial empirical regression equations for different band combinations. The R^2 value for each combination was also determined. The best fitting model is highlighted.

TABLE 5.4- SAMPLE POINTS LOCATION AND TSS CONCENTRATION

SAMPLE	LATITUDE	LONGITUDE	TSS(mg/l)
1	$13^0$24′51.4656″	$80^0$19′13.7958″	117
2	$13^0$25′12.9468″	$80^0$19′16.2048″	40
3	$13^0$25′19.9704″	$80^0$19′14.685″	34
4	$13^0$25′30.3168″	$80^0$19′5.811″	46
5	$13^0$26′17.991″	$80^0$19′5.682″	24
6	$13^0$25′54.8358″	$80^0$18′48.3078″	11
7	$13^0$25′45.3246″	$80^0$18′28.4976″	50
8	$13^0$25′47.1354″	$80^0$18′14.7702″	59
9	$13^0$26′10.1826″	$80^0$18′2.2314″	38
10	$13^0$26′36.405″	$80^0$17′46.88599″	83
11	$13^0$25′16.179″	$80^0$19′4.3602″	79
12	$13^0$27′17.225″	$80^0$17′10.4928″	29
13	$13^0$29′31.4802″	$80^0$15′31.7448″	29
14	$13^0$30′27.039″	$80^0$14′25.461″	19
15	$13^0$31′44.3964″	$80^0$13′59.772″	70
16	$13^0$32′46.2294″	$80^0$13′26.331″	68
17	$13^0$32′41.8662″	$80^0$11’53.8404″	102
18	$13^0$32′30.7818″	$80^0$10′40.0008″	68
19	$13^0$32′29.439″	$80^0$9′6.6018″	162
20	$13^0$31′24.5098″	$80^0$8′25.62″	109
21	$13^0$30′55.8792″	$80^0$8′13.8264″	82
22	$13^0$30′40.2516″	$80^0$9′29.0808″	64
23	$13^0$30′7.7862″	$80^0$10′14.1378″	105
24	$13^0$29′55.9422″	$80^0$10’30.8562″	56
25	$13^0$30′6.3498″	$80^0$10′58.944″	62
26	$13^0$30′0″	$80^0$11′43.1658″	20
27	$13^0$29′54.69″	$80^0$12′33.789″	10
28	$13^0$30′6.336″	$80^0$13′26.5326″	9
29	$13^0$29′26.3358″	$80^0$15′23.4576″	26
30	$13^0$28′5.0658″	$80^0$15′55.1982″	53
31	$13^0$28′17.8716″	$80^0$16′16.6614″	25
32	$13^0$27′29.451″	$80^0$16′45.4188″	43

TABLE 5.5- REGRESSION EQUATIONS FOR 6TH ORDER POLYNOMIAL FIT

S.NO	BAND COMBINATION	REGRESSION EQUATION	R^2 VALUE
1	B1+B11	$y = 1E\text{-}10x^6 - 5E\text{-}08x^5 + 9E\text{-}06x^4 - 0.0008x^3 + 0.0339x^2 - 0.5806x + 143.6$	0.7599
2	B1+B2	$y = 2E\text{-}10x^6 - 8E\text{-}08x^5 + 1E\text{-}05x^4 - 0.001x^3 + 0.0438x^2 - 0.6372x + 128.76$	0.6937
3	B1+B4	$y = 3E\text{-}10x^6 - 1E\text{-}07x^5 + 2E\text{-}05x^4 - 0.002x^3 + 0.0844x^2 - 1.2873x + 125.11$	0.7561
4	B1+B8	$y = -6E\text{-}11x^6 + 2E\text{-}08x^5 - 3E\text{-}06x^4 + 0.0002x^3 + 0.0009x^2 + 0.0944x + 120.69$	0.765
5	B1+B9	$y = 2E\text{-}10x^6 - 7E\text{-}08x^5 + 1E\text{-}05x^4 - 0.001x^3 + 0.04x^2 - 0.6507x + 132.85$	0.7156
6	B1+B2+B3	$y = 9E\text{-}10x^6 - 4E\text{-}07x^5 + 6E\text{-}05x^4 - 0.0052x^3 + 0.2241x^2 - 3.5844x + 36.385$	0.693
7	B3+B5	$y = 4E\text{-}11x^6 + 2E\text{-}09x^5 - 4E\text{-}06x^4 + 0.0005x^3 - 0.0283x^2 + 0.7765x + 78.339$	0.6744
8	B2+B10	$y = 7E\text{-}12x^6 - 4E\text{-}09x^5 + 1E\text{-}06x^4 - 0.0001x^3 + 0.0095x^2 - 0.1658x + 144.67$	0.801
9	B2+B3+B4	$y = 8E\text{-}10x^6 - 4E\text{-}07x^5 + 6E\text{-}05x^4 - 0.0051x^3 + 0.2172x^2 - 3.3244x + 33.374$	0.724
10	B2+B4	$y = 3E\text{-}10x^6 - 1E\text{-}07x^5 + 2E\text{-}05x^4 - 0.0019x^3 + 0.0784x^2 - 1.1415x + 122.09$	0.7639
11	B2+B4+B5	$y = 2E\text{-}10x^6 - 6E\text{-}08x^5 + 4E\text{-}06x^4 + 9E\text{-}05x^3 - 0.0184x^2 + 1.0285x - 0.4505$	0.6956
12	**B2+B7+B8**	$\mathbf{y = -1E\text{-}09x^6 + 6E\text{-}07x^5 - 0.0001x^4 + 0.0076x^3 - 0.2781x^2 + 4.9901x - 18.723}$	**0.8417**
13	B2+B8	$y = -1E\text{-}10x^6 + 4E\text{-}08x^5 - 6E\text{-}06x^4 + 0.0004x^3 - 0.0079x^2 + 0.3089x + 117.14$	0.7588

14	B2+B8+B9	$y = -1E\text{-}10x^6 + 5E\text{-}08x^5 - 9E\text{-}06x^4 + 0.0006x^3 - 0.0187x^2 + 0.4371x + 120.16$	0.762
15	B2+B9	$y = 2E\text{-}10x^6 - 7E\text{-}08x^5 + 1E\text{-}05x^4 - 0.0011x^3 + 0.0455x^2 - 0.7281x + 131.55$	0.6972
16	B3+B11	$y = 9E\text{-}11x^6 - 4E\text{-}08x^5 + 7E\text{-}06x^4 - 0.0006x^3 + 0.026x^2 - 0.4145x + 135.84$	0.7505
17	B3+B4	$y = 4E\text{-}10x^6 - 2E\text{-}07x^5 + 3E\text{-}05x^4 - 0.0024x^3 + 0.1015x^2 - 1.5328x + 120.05$	0.7363
18	B3+B4+B5	$y = -7E\text{-}11x^6 + 5E\text{-}08x^5 - 1E\text{-}05x^4 + 0.0012x^3 - 0.0532x^2 + 1.2854x - 2.7149$	0.6728
19	B3+B6+B7	$y = -7E\text{-}11x^6 + 5E\text{-}08x^5 - 1E\text{-}05x^4 + 0.0012x^3 - 0.0532x^2 + 1.2854x - 2.7149$	0.6728
20	B3+B7	$y = 1E\text{-}11x^6 + 5E\text{-}09x^5 - 3E\text{-}06x^4 + 0.0003x^3 - 0.011x^2 + 0.3724x + 95.86$	0.7542
21	B4+B11	$y = 5E\text{-}12x^6 - 3E\text{-}09x^5 + 8E\text{-}07x^4 - 0.0001x^3 + 0.0057x^2 - 0.0044x + 130.59$	0.791
22	B4+B8	$y = -2E\text{-}10x^6 + 7E\text{-}08x^5 - 1E\text{-}05x^4 + 0.0006x^3 - 0.0122x^2 + 0.4149x + 107.71$	0.7911
23	B4+B8+B9	$y = -3E\text{-}10x^6 + 1E\text{-}07x^5 - 2E\text{-}05x^4 + 0.0011x^3 - 0.0347x^2 + 0.7529x + 111.53$	0.7926
24	B6+B8	$y = -2E\text{-}09x^6 + 9E\text{-}07x^5 - 0.0001x^4 + 0.0109x^3 - 0.4051x^2 + 7.0496x - 30.374$	0.8146
25	B6+B8+B9	$y = -2E\text{-}09x^6 + 9E\text{-}07x^5 - 0.0001x^4 + 0.011x^3 - 0.4125x^2 + 7.2365x - 35.581$	0.8175

The scatter plot of the best fitting 6^{th} order empirical regression model between the measured TSS from laboratory analysis and Landsat 8 OLI/ TIRS band DN values is shown in the Figure 5.4.

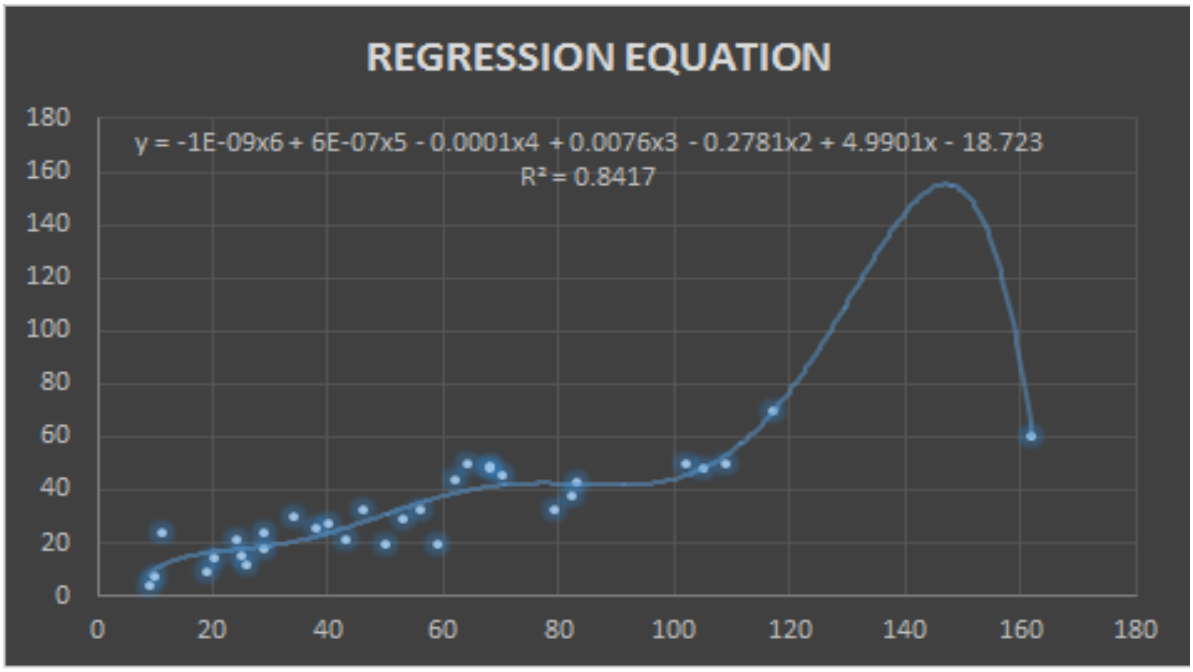

Fig 5.4--Best Fitting 6th Order Empirical Equation

The correlation co-efficient is high for the 6th order polynomial regression equations when compared to linear or other lower orders. The best fit model is obtained for the band combinations 2 + 7 + 8. The R^2 value for the obtained best fit is 0.8417. Polynomial regression between the measured total suspended solids addition of DN values of Blue, SWIR 2 and PAN gives best results. The TSS is calculated for Pulicat Lake using the following empirical equation.

$TSS = [(-1*10^{-9}x^6) + (6*10^{-7}x^5) - (0.0001x^4) + (0.0076x^3) - (0.278x^2) + (4.9901x) - 18.723]$

Where x = Band 2 + Band 7 + Band 8

5.6 SPATIAL DISTRIBUTION MAP OF PULICAT LAKE

A spatial distribution is the arrangement of a phenomenon across the Earth's surface and a graphical display of such an arrangement is an important tool in geographical and environmental statistics. A graphical display of a spatial distribution may summarize raw data directly or may reflect the outcome of more sophisticated data analysis. Many different aspects of a phenomenon can be shown in a single graphical display by using a suitable choice of different colours to represent differences.

Landsat 8 OLI/TIR data was downloaded and proceeded for the months of April and October in 2015, April and September in 2016 and September in 2014. The spatial distribution map of Total suspended solids in Pulicat Lake was produced using polynomial regression model of degree six.

The sixth order regression model which was obtained was applied to the above mentioned data using the Band math option available in ENVI software. The resulted image was enhanced by linear stretch. This enhanced image gives the concentration of total suspended sediments in milligram per litre at each location. The spatial distribution map was created in ArcMap environment.

Figure 5.5 shows the spatial distribution of TSS in April 2015.The results shows that the concentration of the TSS is higher near the inlets of the rivers Arani, Swarnamukhi and Kalanji. The TSS ranges from 250 to 450 mg/l in the northern part of the lake. The TSS ranges from 450 to 600 mg/l in the southern part of the lake. It ranges from 0.0000001 to 250 mg/l in the center of the lake.

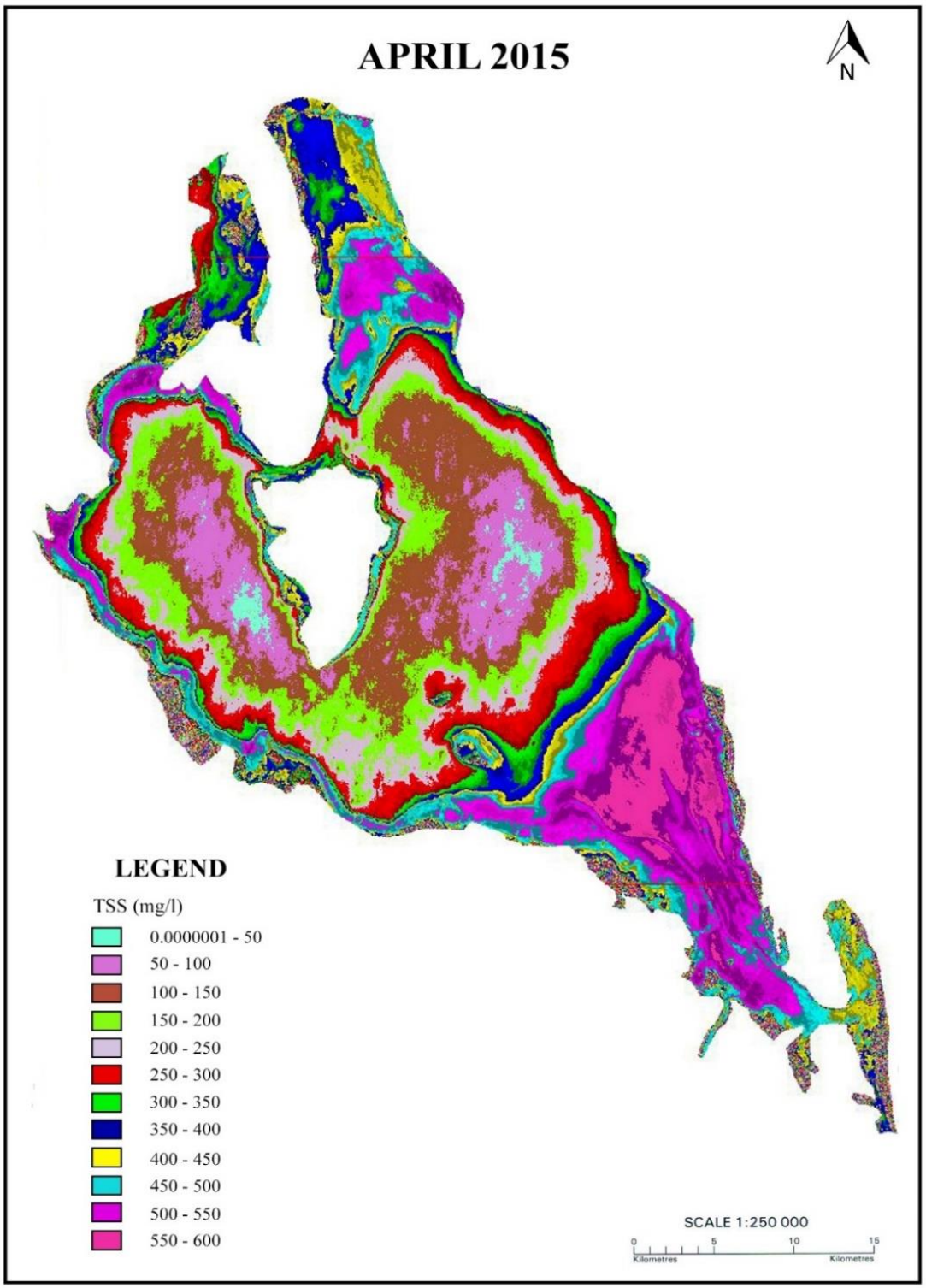

Fig 5.5- Spatial Distribution of TSS for April 2015

Figure 5.6 gives the spatial distribution map of October 2015. The results show that the concentration of TSS is higher at the rim of the lake especially near the three inlets. The concentration of TSS ranges from 0.0000001 to 250 mg/l in the northern part of the lake. The concentration of TSS ranges from 250 to 400 mg/l in the center part of the lake. The TSS ranges from 400 to 600 mg/l in the southern part of the lake.

Figure 5.7 shows the spatial distribution of Total suspended solids of the month April 2016. The result provides evidence for the churning activity on the day of data acquisition. The churning activity is the reason for the dispersed occurrence of TSS concentration. The TSS concentration in the middle of the lake ranges between 0.0000001 and 350 mg/l. The TSS concentration in the southern part of the lake is about 450 to 600 mg/l.

COMPARISON OF THE IMAGES

It can be observed that the region occupied by high TSS concentration in April 2015 is larger than in October 2015. This dilution of TSS concentration in Oct 2015 is due to the mild showers that occurred in the region. From April 2016, it is evident that the churning activity has led to the dispersion of high TSS concentration in the lake.

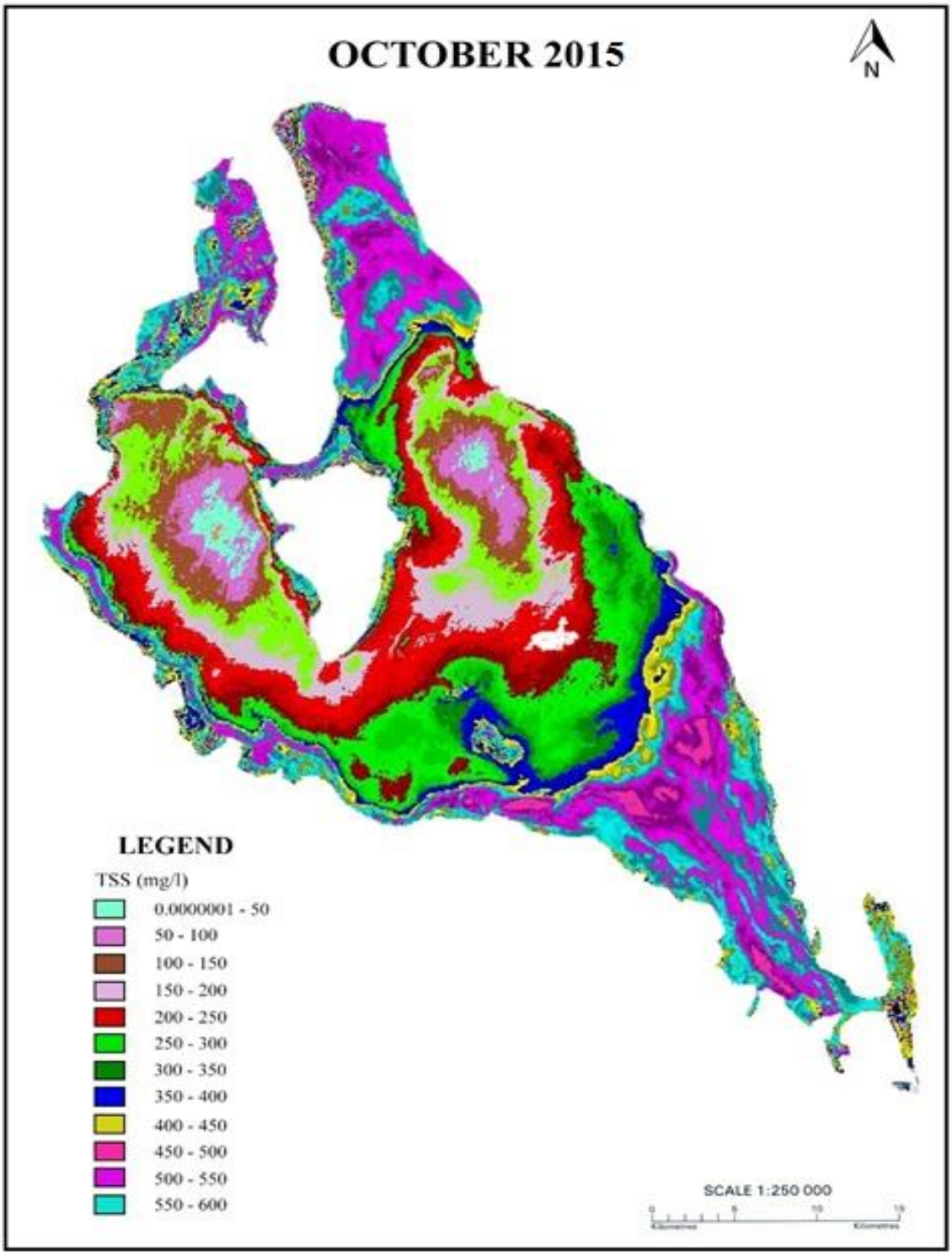

Fig 5.6- Spatial Distribution of TSS for October 2015

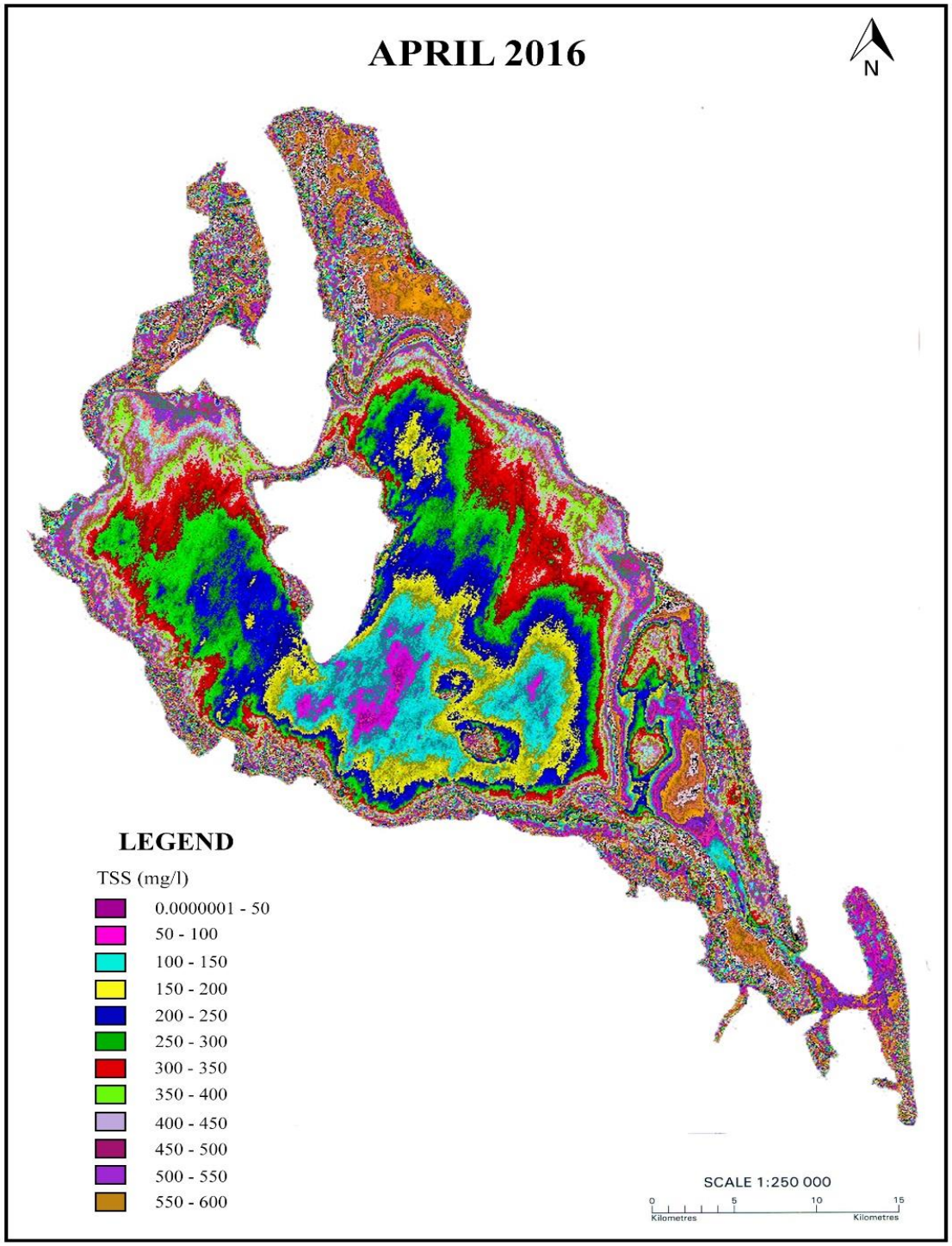

Fig.5.7- Spatial Distribution of TSS for April 2016

CHAPTER 6

CONCLUSION

6.1 SUMMARY

From the laboratory analysis, concentration of total suspended solids in the Pulicat Lake ranges from 9mg/l to 162 mg/l. Many regression models have been developed by correlating total suspended solids from laboratory analysis and DN value/indices of satellite image. Results showed that addition of blue, SWIR 2 and PAN has higher correlation coefficient (0.8417).

Even though the contaminants flow into lake during monsoon season, the total suspended solids reduced due to heavy rain and high inflow of seawater in that season. Density of total suspended solids becomes diluted with rainfall during monsoon season. This causes less TSS value in monsoon season. Temperature of the Pulicat Lake is around 35ºC in surface water during summer season. Concentration of total suspended solids increases due to evaporation water due to heavy temperature and reduction of tidal inflow to the lake.

Tupilipalem sea mouth was silted completely and closed due to reduction of tidal inflow. This reduces movement of water in this region. Due to this reason, northern region has higher concentration of total suspended solids in Pulicat Lake

Recent year's spatial distribution map of 2015 and 2016 has been compared. Result shows that the concentration of total suspended solids is gradually increasing every year. It causes the reduction in depth and area of Pulicat Lake. The sea mouths at Tupilipalem, Rayadoruvu and Pulicat Village of Pulicat Lake,

is gradually closing with sand bar formation due to blow of north bound wind. The sea mouths of Pulicat Lake are not simply a passage, but also a life supporting biocorridor for migration of fishes, crustaceans after spawning in sea and migration after breeding in brackish water lake and vice versa. This important chrono ecological process is basic requirement for making available food for long distant migratory birds, local migrants, but also 50,000 fishermen who are dependent on this lake spread in 600 sq. km.

6.2 RECOMMENDATIONS

The following recommendations for reducing level of siltation have been suggested:

1. Construction of a groyne or tidal inlet wall or an appropriate stone wall or concrete wall or heap of stones to be decided by an Ocean engineer is recommended for three sea mouths to prevent sea mouth closure by sand deposition.
2. Sea mouth dredging and silt removal without loss of molluscans and lake submerged weeds and groyne or wall construction would enhance food availability and biodiversity due to flow of water.
3. The 9.5 km Earthen road bridge built on Pulicat Lake shallow water region known as Attakanithippa needs regular pillar supported bridge with free flow of water.
4. Plantation of mangroves on littoral region.
5. Disposal of effluent from shrimp farms and industries with proper treatment.

6.3 SCOPE OF FUTURE WORK

Total suspended solids value is significantly increasing every year in Pulicat Lake due to contamination. Regression model between the in situ total suspended solids and corresponding pixel DN has given the result with a correlation coefficient of 0.8417. In future accuracy of determination of TSS can be improved using other methods. Prediction of concentration of TSS in the lake using several decades of satellite data and other remote sensing techniques could be developed.

.

REFERENCES

1. Chunlei Fan (2014) ‘ Spectral Analysis of Water Reflectance for Hyper spectral Remote Sensing of Water Quality in Estuarine Water’, *Journal of Geo Science and Environmental Protection, Vol. 2 ,pp 19-27*

2. Dekker A.G, Zamurovie Nenad, Hoogenboom and Peters S.W.M (1996), ‘ Remote Sensing Ecological Water Quality modeling and in situ measurements, a case study in shallow lakes’, *Hydrological Sciences and management, Vol 4, pp 531- 547*

3. Dekkera A.G., Vosb R.J. Peters S.W.M (2001), ‘ Comparison of remote sensing data, model results and in situ data for total suspended matter TSM in the southern Frisian lakes’, *The Science of the Total Environment, Vol.268, pp 197-214*

4. Hellweger F.L, Schlossera P,Lall U, and Weissel Estuarine J.K (2004), ‘ Use of satellite imagery for water quality studies in New York Habor’, *Coastal and Shelf Science, Vol.61, pp 437- 448*

5. Yirgalem Chebud, Ghinwa M. Naja, Rosanna G. Rivero and Assefa M. Melesse (2012), ‘Water Quality monitoring using remote sensing and Artificial neural network’, *Water, air, soil pollution management Vol.223, pp 4875-4887*

6. Nanda Kumar N V, Ngarjuna A, and Reddy D C(2010), 'Ecoresiliency and Remediation Strategies for Biodiversity Conservation of Aquatic and Avifauna of Pulicat Brackish Water Lagoon', Department of Fishery Science and Aquaculture, *World journal of Fsh and Marine Science, pp 389-400.*

7. Korandi M, Gy. Buttner, Geomorei A and Zs. Kote (1987). "Satellite Remote Sensing of Inland Waters': *Lake Balaton And Reservoir Kiskore, Research Centre For Water Resource Development*, Vol. 15, pp. 305-311.

8. Lijuan Cui, Yue Qiu, Teng Fei, Yaolin Liu & Guofeng Wu (2013), 'Using Remotly sensed suspended sediment concentration variation to improve management of Poyang Lake', *Lake and Reservoir Management,*Vol.29:1, pp.47-60.

9. Lim H.S, MatJafri M.Z, Abullah K, Tan K.C, Tan. F, Mohd. Saleh N,, Yasin2 Z and Abullah A.L (2009), 'Monitoring of Total Suspended Solids and Sea Surface Temperature using NOAA – AVHRR Data in Malaysia, *MASAUM Journal of Basic and Applied Sciences'*, Vol. 1, pp., 395-40.

10. Mithuthapala/, Sriyanie (2013), 'Lagoons and Estuaries', *Coastal Ecosystems Series, IUCN Sri Lanka Country Office, Colombo*, Vol 4, pp.**No index entries found.** 73.

11. Sundheer K.p, Indrajeet Chaubey, and Vijay Garg (2006), 'Lake Water Quality Assessment from Landsat Thematic Mapper Data Using Neutral Network: An Approach to Optimal Band Combination Selection', *Journal of the American Water Resources Association*, pp.1683 – 1695.

12. Weiqi HE, Shan CHEN, Xuehua LIU, Jining CHEN (2008), 'Water Quality Monitoring in slightly-polluted inland water body through Remote Sensing- A case study in Guanting Reservoir, Beijing', *Journal of Environmental Sciences of Engineering*.